Progress in Physics of Applied Materials 6 (2026), Serial Number 11, 137–149

Semnan University

Progress in Physics of Applied Materials

journal homepage: https://ppam.semnan.ac.ir/

Sustainable Gold Nanoparticles Possessed Significant Activity Against Cancer Cell Lines (MCF-7, HeLa, and A549)

Ajay Kumar[a*], Manish Pant[b], Dhruv Mishra[c], Gurleen Kaur[d], Dharmendra Kumar [e], Rupinder Kaur[f], Benjamin K. Blamah[g], Narinder Kumar[h], Sarvesh Rustagi[i,j*], Devendra Singh[i]

[a]*Department of Chemistry, School of Applied and Life Sciences, Uttaranchal Institute of Technology, Uttaranchal University, Dehradun, 248007, Uttarakhand, India*
[b]*Department of Chemical Engineering, IISER Bhopal, 462066, Madhya Pradesh, India*
[c]*Department of Biological Sciences, College of Basic Sciences and Humanities, G.B. Pant University of Agriculture and Technology, Pantnagar, Uttarakhand (U.K.), India-263145*
[d]*Department of Applied Science and Humanities, Tula's Institute, Dehradun-(UK)-248001, India*
[e]*School of Engineering and Computing, Dev Bhoomi Uttarakhand University, Dehradun*
[f]*Department of Agriculture, Tula's Institute, Dehradun (UK)-248001, India*
[g]*Living Water International, NGO, Faith-based, Houston, Taxes, USA*
[h]*Department of Physics, UIT, Uttaranchal University, Dehradun, Uttarakhand, India- 248007*
[i]*School of Agriculture and Technology, Maya Devi University, Dehradun, Uttarakhand, India*
[j]*Department of Life Sciences, School of Bioscience and Technology. Galgotias University, Greater*

ARTICLE INFO

Article history:
Received: 6 October 2025
Revised: 8 November 2025
Accepted: 15 November 2025
Published online: 3 December 2025

Keywords:
Gold nanoparticles (GNPs);
Leucas cephalotes (*Lc*);
Characterization;
Anticancer activity;
Breast;
Lung, Cervical;
Cancer cell lines.

ABSTRACT

Nanoparticles (NPs) have begun substituting for more conventional cancer treatments in contemporary oncology, including radiation, chemotherapy, and surgery. Gold nanoparticles (GNPs) synthesized using *Leucas cephalotes (Lc*) leaf extract were developed via a green, eco-friendly route and evaluated for their anticancer potential. The formation of *Leucas cephalotes*–gold nanoparticles (*Lc*-GNPs) was confirmed by a distinct surface plasmon resonance peak at 524 nm, while XRD analysis revealed four prominent diffraction peaks, indicating their crystalline nature. SEM showed the spherical morphology and interaction of *Lc*-GNPs against cancer cell lines, and DLS revealed an average particle size of 20 nm with a narrow size distribution. Cytotoxic studies revealed dose-dependent inhibition of cancer cell viability, with IC_{50} values of 26.91 µg/mL (MCF-7 breast cancer), 45.51 µg/mL (HeLa cervical cancer), and 17.33 µg/mL (A549 lung cancer). *Lc*-GNPs activity is statistically significant against all three MCF-7, HeLa, and A549 cancer cell lines. *Lc*-GNPs cancer activity compared with standard chemotherapeutic agents, literature-reported GNPs, and their combination. The *Lc*-GNPs demonstrated moderate potency but significantly lower expected systemic toxicity. These results indicate that *Lc*-derived GNPs possess promising, quantifiable anticancer efficacy and can serve as a sustainable nano biocompatible cancer therapeutic. The IC_{50} values were determined from dose–response curves using nonlinear regression analysis. A549 cells exhibit the lowest viability and the highest cytotoxic response, confirming that *Lc*-GNPs possess the greatest potency against the A549 lung cancer cell line, followed by MCF-7 cells and HeLa.

1. Introduction

Cancer remains one of the leading causes of mortality worldwide, and conventional treatment strategies such as chemotherapy, radiation therapy, and surgery have been the primary approaches for treating cancer, a disease characterized by uncontrolled cell proliferation and

* Corresponding author.
E-mail address: ajay.tiwari1591@gmail.com, sarveshrustagi@gmail.com

Cite this article as:
Kumar, A., Pant, M., Mishra, D., Kaur, G., Kumar, D., Kaur, R., Blamah, B.K. Kumar, N., Rustagi, S. and Singh, D., 2026. Sustainable Gold Nanoparticles Possessed Significant Activity Against Cancer Cell Lines (MCF-7, HeLa, and A549). *Progress in Physics of Applied Materials*, *6*(2), pp.137-149. DOI: **10.22075/ppam.2025.39282.1175**

differentiation [1]. Nanotechnology has emerged as a transformative approach for overcoming these limitations by enabling targeted drug delivery, real-time diagnosis, and multifunctional therapeutic interventions. Although these therapies are effective in killing cancer cells, they also cause numerous adverse side effects due to their non-specific action on healthy tissues [2]. Recent advancements in nanomedicine (NM), targeted drug delivery, and multi-target inhibitors have rendered these traditional cancer treatment modalities increasingly outdated [3]. Both metal and non-metal nanoparticles (NPs) are extensively explored in NM, a branch of nanotechnology focused on the biomedical treatment of disease. NM holds significant promise for early cancer detection and therapy owing to its advanced imaging, therapeutic capabilities, and the ability to target tumor tissue through both passive and active mechanisms. Inorganic NPs form the backbone of NM; several inorganic NP-based formulations conjugated with anticancer drugs or bioactive substances, such as peptides, proteins, and DNA, have already been approved by the U.S. Food and Drug Administration (FDA) and European regulatory agencies, including Feridex, Resovist, Doxil, and Abraxane [4]. Compared to conventional cancer therapeutics, these nanomedicines offer enhanced solubility/bioavailability, biocompatibility, and multi-functionality [5]. Furthermore, the selective cytotoxicity of inorganic NPs toward cancer cells has been well established [6].

Inorganic NPs widely used in anticancer therapy include iron oxide (Fe_2O_3 and Fe_3O_4) [7], titanium dioxide (TiO_2), cerium oxide (CeO_2), zinc oxide (ZnO), copper oxide (CuO), and silica (SiO_2), among others [8,9]. Their unique physicochemical properties make them highly effective tools for cancer treatment. For instance, Fe_2O_3 NPs conjugated with anticancer drugs are used to create magneto-sensitive systems for selective targeting using external magnetic fields [10]. TiO_2 NPs are widely used in photodynamic therapy, where they generate reactive oxygen species (ROS) upon radiation exposure without requiring additional photosensitizers to induce apoptosis in tumor cells [11,12]. Despite these advances, concerns persist regarding the safety and toxicity of green-synthesized NPs toward both normal and malignant cells. If metal NPs demonstrate efficient cytotoxicity toward cancer cells than toward normal cells, they hold potential as anticancer agents [13]. Gold nanoparticles (GNPs), in particular, offer significant advantages over other metallic NPs due to their minimal cytotoxicity in human cells. Studies on human leukemia cells have shown that even at high concentrations, spherical GNPs with various surface modifiers exhibit no intrinsic toxicity [14]. GNPs have garnered exceptional interest due to their controlled size-dependent behavior, superior biocompatibility, high physicochemical stability, and distinct optical properties that support imaging, biosensing, and photothermal therapy [15]. Breast cancer remains one of the leading causes of mortality among young women worldwide [16]. These cancers often involve multiple mutations that drive uncontrolled cell proliferation and impair apoptosis, contributing to resistance against conventional therapies. Such challenges underscore the importance of nanotechnology in improving therapeutic efficacy. Numerous studies have shown that the performance and cellular interactions of NPs depend heavily on their synthesis parameters [17].

Tomar and Garg [18] demonstrated the ability of GNPs to cluster within tumor cells and scatter light, enabling their use as probes for microscopic cancer imaging. Owing to their optical properties, GNPs serve as excellent contrast agents in optical and X-ray imaging systems, facilitating the detection of atherosclerotic plaques, fibrous tissues, and intravascular thrombi [19]. GNPs also show therapeutic potential in managing diabetes and associated microvascular complications due to their anti-inflammatory, anti-hyperglycemic, antioxidant, anti-glycation, anti-angiogenic, and anti-fibrotic activities [20]. Additionally, they exhibit notable catalytic activity in the degradation of methylene blue [21]. Metal NPs are commonly synthesized through physical, chemical, and biological methods [22,23]. However, green synthesis has gained considerable attention as an environmentally friendly and cost-effective alternative [24]. Biological systems used in green synthesis include fungi [25], plants [26], and their extracts, as well as microorganisms such as yeast [27] and bacteria [28]. These biological resources offer safe, sustainable, and economically feasible production routes [29], enabling major advancements in biomedical applications [30]. Among these methods, plant-based synthesis is particularly preferred due to its simplicity, safety, one-step processing, and suitability for large-scale operations without generating hazardous by-products [31,32]. Plants also eliminate the need for maintaining bacterial or fungal cultures and long incubation periods [33]. Moreover, plant extracts with inherent therapeutic properties can yield NPs with enhanced biological activity [34].

In this context of green synthesis offers a sustainable alternative to traditional chemical and physical methods, which often require hazardous reducing agents and generate toxic waste. Plant essential oils contain organic substances (alkaloids, terpenoids, etc.) are the core branch of phytochemicals. Essential oils serve simultaneously as reducing, capping, and stabilizing agents, thereby governing NPs' morphology, dispersion, and surface chemistry [35, 36]. Despite rapid advancements in the field, limited studies have systematically examined how the phytochemical richness of a specific plant species influences the anticancer performance of the synthesized nanoparticles [37].

2. Molecular Mechanics

GNPs have demonstrated significant anticancer activity against various cancer cell lines, including MCF-7, HeLa, and A549 cancerous cell lines [38]. Their effectiveness is attributed to several mechanisms and has been validated in multiple recent studies. Gold nanoclusters (GNCs) are emerging agents in cancer treatment, including for breast and lung cancers, due to their unique physicochemical properties and ability to be functionalized with targeting ligands or drugs [39] (Figure 1). Molecular docking studies are frequently used to predict and optimize the interaction of these nanoclusters with cancer-related proteins, often using structures from the Protein Data Bank (PDB) [40].

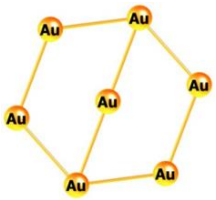

Fig. 1. Gold nanoclusters (GNCs) are used as a promising anticancer agent.

2.1. Cytotoxicity and Selectivity

GNPs synthesized via green methods (using plant extracts or biocompatible agents) show dose-dependent cytotoxicity against MCF-7 (breast), HeLa (cervical), and A549 (lung) cancer cell lines, with minimal toxicity to normal cells. Chitosan-coated gold nanoparticles (Ch-GNPs) selectively induced cell death in HeLa and MCF-7 cells, sparing normal cells [41].

2.2. Mechanistic Insight into Anticancer Activity

The anticancer mechanism of GNPs is primarily attributed to reactive oxygen species (ROS) generation, leading to oxidative stress**,** mitochondrial dysfunction, and activation of caspase-dependent apoptotic pathways [42]. GNP exposure disrupts the mitochondrial membrane potential, releasing pro-apoptotic factors such as cytochrome-c, which activate downstream caspases (e.g., caspase-3 and -9) [43]. Additionally, treatment with GNPs may lead to cell cycle arrest at the G2/M phase and downregulation of anti-apoptotic genes (Bcl-2, PI3K/Akt, mTOR) while upregulating pro-apoptotic genes (Bax, TNF-α). The relatively higher sensitivity of HeLa cells suggests enhanced cellular uptake and internalization of GNPs, possibly due to differential membrane receptor expression [44] (Table 1).

Table 1. GNPs activity against some cancer cell lines.

S.No.	Cancer Cell Line	Mechanisms Observed
1	MCF-7	ROS generation, apoptosis, mitochondrial dysfunction
2	HeLa	ROS generation, apoptosis, and cell cycle arrest
3	A549	Apoptosis, cell cycle arrest, gene regulation

GNPs possessed efficient treatment, moderate cytotoxicity with excellent biocompatibility and minimal expected side effects, making them a sustainable alternative for targeted cancer therapy.

2.3. Enhanced Drug Delivery and Synergy System

GNPs can be functionalized with targeting molecules (e.g., folic acid) or loaded with chemotherapeutics to improve delivery specifically to cancer cells, enhancing efficacy and reducing systemic toxicity [45]. Combination therapies (e.g., GNPs with turmeric or metformin) show synergistic effects, lowering the required effective dose and increasing cancer cell death. Recent advances in GNP research from 2020 to 2025 reveal a clear shift toward targeted, biocompatible, and multifunctional nano-therapeutics for cancer treatment [46-58]. The cytotoxic efficacy of gold standard chemotherapeutic drugs and previously reported green-synthesized GNPs (Table 2). Early studies focused primarily on green-synthesized and biologically mediated GNPs, highlighting their inherent cytotoxicity and ROS-induced apoptotic effects in multiple cancer cell lines.

In years 2023–2025, the field moved toward more engineered and precision-based designs, including PEGylated GNPs, folic acid-functionalized nanoparticles, EGFR-conjugated systems, and phytochemical-loaded GNPs (e.g., curcumin, myricetin). These modifications significantly enhanced selective cellular uptake, stability, and tumor-specific accumulation, while reducing systemic toxicity.

Furthermore, photo-thermal platforms such as gold nanorods demonstrated strong potential for non-invasive treatment. Overall, the trend reflects a progression from simple biogenic nanoparticles to highly tunable and targeted NMs strategies, positioning GNPs as versatile agents for next-generation cancer therapy. Green-synthesized and surface-modified GNPs generally exhibit low toxicity to normal cells and are considered biocompatible in vivo models [59, 60].

Table 2. Study of the therapeutic activity of reported anticancer agents.

S.No.	Therapy/ Nanotechnology	Results	Year	Reference
1	*Padina tetrastromatica* (Marine brown seaweed) GNPs	Anti-cancer activity of GNPs for liver and lung, and breast cancer treatment	2020	[46]
2	Myricetin GNPs	Myr-GNPs act as an effective anticancer medicine.	2020	[47]
3	Gum acacia (Gemcitabine hydrochloride-loaded colloidal GNPs)	The multipurpose way for the development of breast cancer therapy.	2020	[48]
4	Flaxseed (*Linum usitatissimum*) GNPs	The mediated NPs exhibited inhibitory activity against breast cancer, hepatocellular carcinoma, and subsequently, colon carcinoma cell lines	2021	[49]
5	Gold nanorods (GNRs) for photothermal therapy	GNRs showed strong NIR absorption and effectively induced cancer cell death via localized hyperthermia.	2021	[50]
6	PEGylated GNPs	pH-responsive anticancer drug nanoconjugate	2021	[51]
7	Red sea weeds (GNPs)	Anticancer agents against human breast adenocarcinoma	2022	[52]
8	Salvia officinalis GNPs	Human breast (MCF-7) cancer cell line	2023	[53]
9	*Clitoria ternatea* Flower Extract Ag-Au Bimetallic NPs	In-vitro Anticancer Potential	2023	[54]
10	PEGylated GNPs	PEG-GNPs against MCF-7 breast cancer cells	2024	[55]
11	Curcumin (Cur)-GNPs	Cur-GNPs synergistically improved curcumin bioavailability and exhibited strong cytotoxic effects against MCF-7 and HeLa cells through enhanced cellular uptake.	2025	[56]
12	Folic acid (FA)-GNPs	FA-GNPs showed selective targeting of folate receptor–positive breast cancer cells	2025	[57]
13	EGFR antibiotic–GNPs	EGFR–GNPs exhibited precise targeting of EGFR-overexpressing breast and lung cancer cells, with minimal off-target toxicity.	2025	[58]

3. Materials and Methods

3.1. Plant Materials and Extract Preparation

The basic plant identification of leaves from the *Leucas cephalotes* (*Lc*) plant, common name: Guma, collected from the place Motornagar, Johnpur, Kotdwar in the state of Uttarakhand, was aided by the present researchers. Several equipment and materials were employed for the extraction, such as acetone (AR grade) and hydrochloric acid ($HAuC_{l4}$– 1 mM) from Sigma Aldrich, as well as a Soxhlet apparatus, A459 cell lines, a microscope, a CO_2 incubator, and double-distilled water.

The collected leaves were thoroughly washed with double-distilled water to remove residual dust particles and air-dried for 3–5 days at room temperature (25 ± 1°C). The dried leaves were finely ground into powder using a grinding machine. The leaves of this plant were ground into a fine green powder, which was then kept for use in the test. Approximately 8 g of the crude powdered leaves was boiled with 300 mL of deionized water in a 1000 mL round-bottom flask for 1 hour at 85–90°C. The mixture was cooled to room temperature and filtered through Whatman No. 1 filter paper. The resulting yellowish filtrate was stored at 4°C for further use as the reducing and stabilizing agent in the synthesis of the yellow-tinted generated leaf extract, as shown in (Fig. 2).

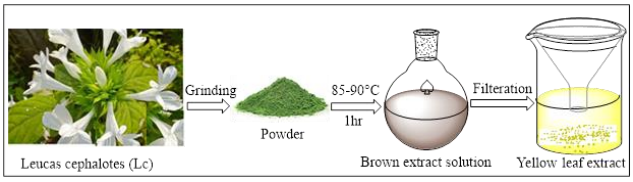

Fig. 2. Preparation of crude GNPs leaf extract from leaves of *Leucas cephalotes (Lc)*.

3.2. Synthesis of Gold nanoparticles (GNPs)

In the synthesis, 12 mL of the *Lc* leaf extract for reducing Au^{3+} ions to Au^0 was added to 60 mL of 1 mM chloroauric acid ($HAuCl_4$) (aq) solution under constant stirring at room temperature. The mixture was incubated for 1 hour at ambient conditions (~25 ± 2°C, pH 7.0) under continuous stirring. The formation of gold nanoparticles was indicated by a color change from pale yellow to ruby red due to surface plasmon resonance (SPR) recorded as a function of time to track the reduction of $AuCl_4$, typically achieved after 2 hours of incubation. The synthesized *Lc*-GNPs were centrifuged at 14,000 rpm for 15 minutes (Eppendorf Centrifuge 5804R, Thermo Fisher Scientific, Germany), 15 minutes spent to remove unreacted materials and large

aggregates. The eluted samples (3.5 mL total) were washed twice with deionized water and redispersed in 10 mM sodium phosphate buffer (pH≈7.0), as the leaf extract served as both a reducing and stabilizing agent (Figure 3). Reaction conditions were optimized by incubation time (24 hours), further extracting the unwanted volume to obtain stable *Lc*-GNPs. The purified *Lc*-GNPs were stored at 4°C for further characterization and biological assays

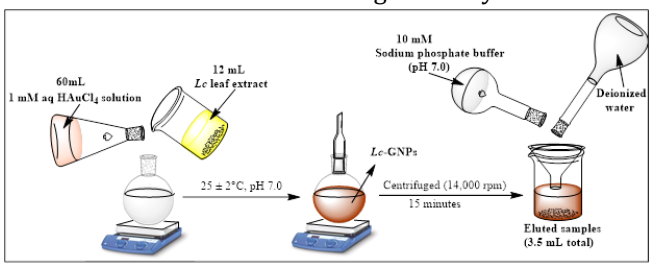

Fig. 3. Flow diagram of synthesis of *Leucas cephalotes* gold nanoparticles (*Lc*-GNPs).

3.3. Characterization of Lc-GNPs

The optical properties of the synthesized *Lc*-GNPs were analyzed using UV–Vis spectroscopy (λ = 400–700 nm range). Dynamic light scattering (DLS) was employed to analyze the size and size distribution of particles less than a micron. Crystallinity was confirmed by X-ray diffraction (XRD) using Cu-Kα radiation (λ = 1.5406 Å), and morphological features were observed through scanning electron microscopy (SEM, JEOL JSM-6390LV). Elemental composition was examined using energy-dispersive X-ray spectroscopy (EDX), while functional groups involved in reduction and stabilization were identified by Fourier-transform infrared spectroscopy (FTIR, 4000–400 cm^{-1}).

3.4. MTS Cytotoxicity Assay

Method: The Mesial temporal sclerosis (MTS) assay is a widely used colorimetric method for assessing cell viability, proliferation, and cytotoxicity. Unlike the MTT assay, MTS is less toxic and produces a water-soluble formazan product, eliminating the need for an additional solubilization step. The assay is based on the bioreduction of the MTS tetrazolium compound by metabolically active cells, resulting in the formation of a colored formazan dye in the culture medium. Cytotoxicity was evaluated according to the manufacturer's protocol using the CellTiter 96® Aqueous One Solution Cell Proliferation Assay (Promega, WI, USA). The assay reagent contains the MTS compound (3-(4,5-dimethylthiazol-2-yl)-5-(3-carboxymethoxyphenyl)-2-(4-sulfonyl)-2H-tetrazolium) and the electron-coupling reagent phenazine ethosulfate (PES) premixed in a single solution. A549, HeLa, and MCF-7 cells were seeded into 96-well plates at a density of 5,000 cells/well and incubated for 24 h to allow attachment. The medium was then replaced with fresh culture medium containing poly-(triethylamine ester) (PTAE) with GNPs at graded concentrations of 100, 33.33, 11.11, 3.70, 1.23, and 0.41 µg/mL. Control wells received complete medium without any treatment [61.62].

3.5. Dose–Response

The cytotoxicity data obtained from the MTS assay were modeled using a four-parameter logistic (4PL) sigmoidal equation to describe the dose–response relationship between *Lc*-GNP concentration and cancer cell viability [63]. This model accounts for the asymptotic behavior of cell responses at both low and high concentrations and provides a robust estimation of the IC_{50} value, the concentration required to reduce cell viability by 50% [64]. The general form of the 4PL equation is:

$$Y = \text{Bottom} + \text{Top-Bottom}/\ 1 + (X/IC_{50})^{\text{Hill Slope}}$$

where *Y* represents the predicted cell viability (%), *X* is the nanoparticle concentration (µg/mL), *Bottom* and *Top* correspond to the minimum and maximum asymptotic responses, and the *Hill slope* determines the steepness of the curve.

4. Results and Discussion

4.1. Surface Plasmon Resonance (SPR)

Primary verification for the green production of GNPs using *Lc* extract came from visual inspection. The reaction mixture (*Lc* extract + 1 mM $HAuCl_4$) turned ruby red after 24 hours. The *Lc* extract initially had a light yellow colour. Surface plasmon resonance (SPR) is associated with this color shift, which signifies the completion of the reduction process, absorbance (a.u.), and wavelength (nm) [65, 66]. The **UV–Vis SPR peak at 524 nm** confirms the reduction of Au^{3+} to Au^0, indicating electron donation by phenolic and flavonoid constituents of *Lc-plant extract* (Fig. 4) [67].

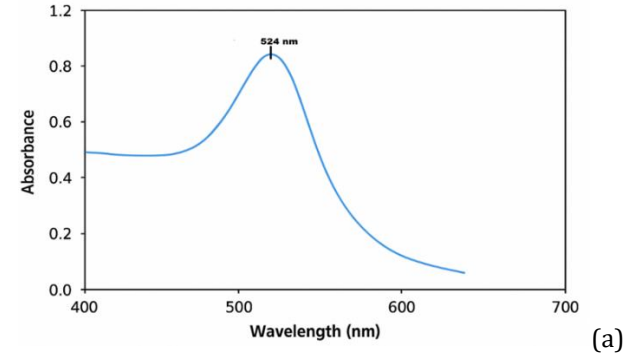

(a)

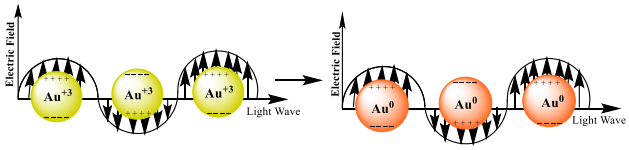

(b)

Fig. 4. (a) UV-Vis absorption spectrum of *Lc*-GNPs, (b) Schematic propagating SPR of *Lc*-GNPs.

4.2. Fourier-transform infrared spectroscopy (FTIR)

Fourier-transform infrared spectroscopy (FTIR) of both the *Lc* extract and Lc-GNPs revealed several functional groups responsible for nanoparticle synthesis and stabilization. Prominent peaks at 3420 cm^{-1} (–OH stretching), 1635 cm^{-1} (C=O stretching), and 1380 cm^{-1} (C–

N stretching) correspond to polyphenols, flavonoids, and proteins. These biomolecules likely act as reducing electrostatic and hydrogen-bond interactions. This mechanism aligns with established models of green nanoparticle synthesis, where plant-derived phenolics and terpenoids provide the necessary electrons for metal ion reduction while maintaining colloidal stability [68].

4.3. Dynamic light scattering (DLS)

Dynamic light scattering (DLS), the size and size distribution of particles less than a micron can be analyzed using DLS. The particles are suspended in a laser beam that illuminates them to measure the Brownian motion velocity and calculate their size, which is the maximum frequency (peak) that occurs around 20 nm, the average hydrodynamic diameter of the GNPs. The fluctuation of scattered light is then tracked and evaluated. When it comes to measuring the size of particles, assessing surface modification, tracking the stability of GNPs over time, and detecting approaches for bio-assays, DLS measurement of GNPs is a very sensitive technique (Fig. 5).

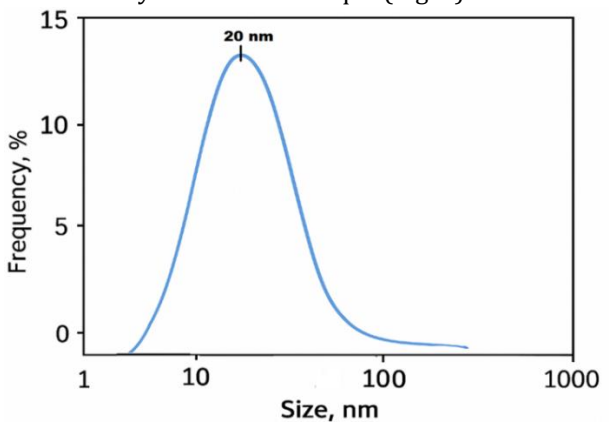

Fig. 5. DLS measures the average particle size of GNPs.

4.4. X-ray Diffraction Analysis

The powdered GNPs were examined using XRD, and distinct peaks of cubic phases (JCPDS No. 03-0921) were found at exhibiting distinct diffraction peaks at 2θ values of 38.2°, 44.3°, 64.9°, and 77.5°, corresponding to the (111), (200), (220), and (311) planes of face-centered cubic (fcc) gold, respectively. These findings demonstrate that GNPs are crystalline. The enormous bottom breadth of the peaks provides indirect evidence of the formation of smaller-sized GNPs. Figure 6 shows the results of the XRD pattern of the GNPs.

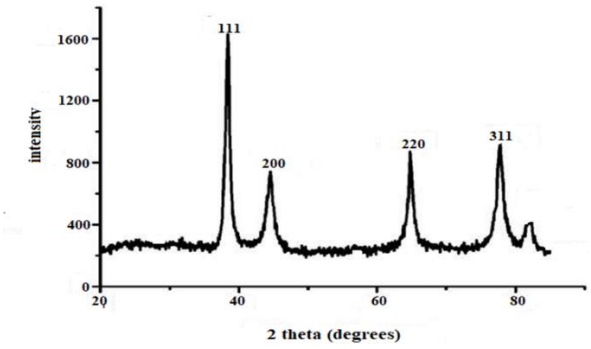

Fig. 6. X-ray diffraction pattern showing characteristic peaks corresponding to crystalline gold.

4.5. SEM Analysis

SEM image of *Lc*-derived GNPs has demonstrated that the GNPs possess a predominantly spherical morphology with smooth surface texture and uniform distribution, strong anticancer efficacy against A549 cancer cells, at concentrations of dose-dependent activity against lung cancer cells at distinct dosages. Cells were treated with varying concentrations of *Lc*-GNPs (0.41–257.8 µg/mL) for 72 hours. The highest concentration dose (257.8 µg/mL) of *Lc*-GNPs exhibits the strongest anticancer activity against A549 lung cancer cell lines (Fig. 7).

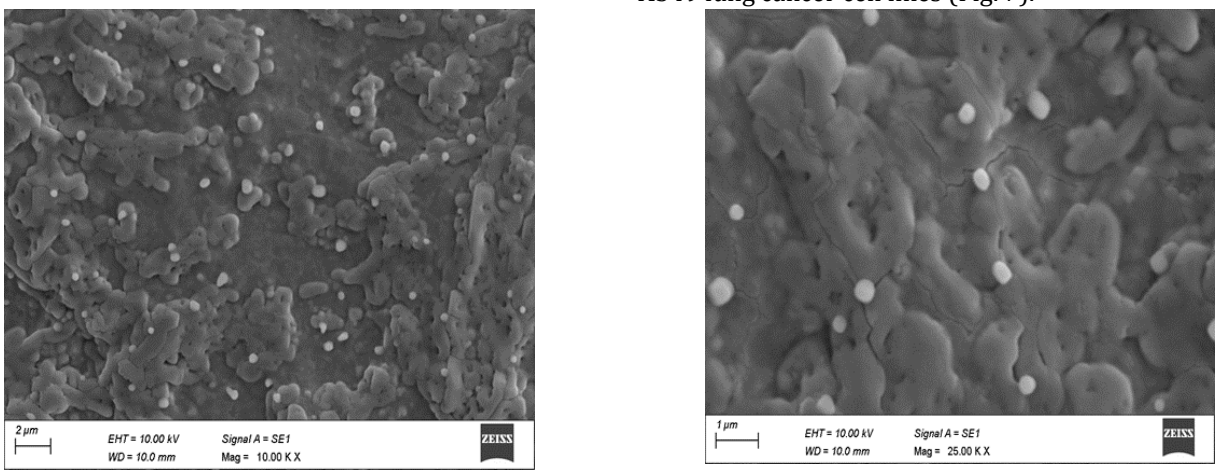

Fig. 7. SEM micrograph showing spherical, well-dispersed *Lc*-GNPs on A549 lung cancer cell lines.

At a maximum dosage of 257.8 µg/mL, the study found that these GNPs had a significant cytotoxic effect on A-549 cancer cells. Small-sized NPs generally penetrate deeply into cancer tissue and perform efficiently, rather than larger-sized NPs, demonstrating the size-dependent nature of NPs and their anticancer effect.

4.6. Energy Dispersive X-ray (EDX)

The elemental composition of the synthesized *Lc*-GNPs was confirmed through EDX spectroscopy. The EDX spectrum displayed a strong, **broad** gold signal at **2.2 keV**, which corresponds to the characteristic energy peak of

metallic gold, validating the successful formation of GNPs. In addition to the gold broad peak, silicon (Si) intense peaks at 1.74 keV were also observed (Fig. 8).

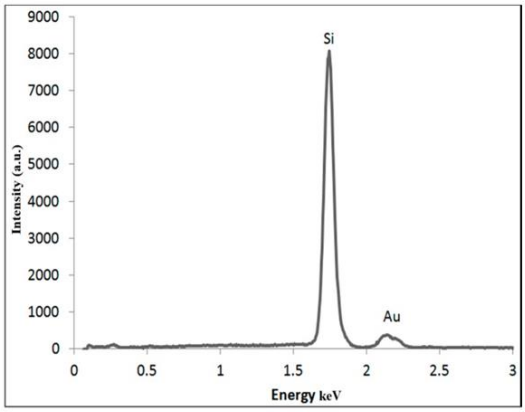

Fig. 8. EDX spectrum of *Lc*-GNPs extract.

Minor peaks corresponding to carbon (C) peak at 0.27 keV and oxygen (O) are negligible, which indicates the presence of phytochemical residues from the plant extract, which act as natural reducing and capping agents during nanoparticle synthesis. Silicon (Si) intense signals are typically attributed to the biomolecules from the *Lc* extract that act as reducing and stabilizing agents during nanoparticle synthesis. Overall, the EDX analysis confirms the successful bioreduction of Au^{3+} ions to Au^0 nanoparticles and validates the elemental purity and organic coating derived from the *Lc* extract.

4.7. Cytotoxicity Assessment and Statistical Analysis

Cells were treated with varying concentrations of *Lc*-GNPs (0.41–257.8 µg/mL) for 72 hours. Cell viability (%) was determined relative to untreated controls using the Cell Titer 96® Aqueous One Solution assay (Promega, USA). The cytotoxic activity of *Lc*-GNPs was assessed using the MTS assay against MCF-7, HeLa, and A549 cell lines following 72 h of incubation at 37 °C in 5% CO_2. The medium was removed, and cells were gently washed twice with sterile phosphate-based buffer solution (PBS). Subsequently, 20 µL of MTS reagent (0.5 mg/mL) was added to each well and incubated for 4 h at 37 °C. After incubation, 100 µL DMSO was added to each well to ensure complete solubilization of the formazan product. Absorbance was recorded in nm with a reference wavelength using a Max 340 microplate reader (Molecular Devices, USA). The assay demonstrated dose-dependent inhibition of cell viability across all three cancer cell lines (MCF-7, HeLa, and A549) was calculated based on the absorbance relative to the untreated control group.

The cell viability results, expressed as mean ± SD from triplicate experiments, demonstrated a clear concentration-dependent decline in cell viability across all tested cell lines (Table 3). At the lowest concentration (0.41 µg/mL), cell viability remained above 90% for all cell lines, indicating negligible cytotoxic effects. However, progressive decreases were observed with increasing concentrations of *Lc*-GNPs. At 33.33 µg/mL, MCF-7, HeLa, and A549 exhibited reduced viabilities of approximately 40.69 ± 4.78%, 55.27 ± 5.11%, and 34.08 ± 3.68%, respectively. The highest concentration (257.8 µg/mL) resulted in significant cytotoxicity, with viability dropping to 6.86 ± 6.15% (MCF-7), 16.52 ± 1.44% (HeLa), and 5.11 ± 1.67% (A549). These results confirm that *Lc*-GNPs induce a concentration-dependent inhibition of cancer cell viability, with the A549 line displaying the highest susceptibility.

The fitted four-parameter logistic (sigmoidal) dose–response curves revealed a characteristic S-shaped inhibition pattern, allowing precise determination of IC_{50} values for each cell line. The model effectively captured the nonlinear cytotoxic response and provided strong correlation coefficients ($R^2 > 0.95$). All experiments were performed in triplicate (n = 3), and results are presented as mean ± SD. Statistical analysis using one-way ANOVA followed by ($p < 0.05$) confirmed significant differences between treated and control groups, and that the reductions in cell viability were statistically significant ($p < 0.05$) at concentrations above 3.70 µg/mL compared with untreated controls. Among the tested cell lines, A549 cells were found to be the most sensitive to *Lc*-GNPs, followed by MCF-7 and HeLa, suggesting variable susceptibility likely related to differences in cellular uptake or oxidative stress response mechanisms (Table 4).

The fitted sigmoidal curves exhibited an excellent agreement with the experimental data for all three cancer cell lines (MCF-7, HeLa, and A549. The regression analysis yielded IC_{50} values of 26.91 µg/mL for MCF-7, 45.51 µg/mL for HeLa, and 17.33 µg/mL for A549. The curve steepness (Hill coefficient) suggested a cooperative cytotoxic response, indicating effective NPs–cell interactions. These results confirm that *Lc*-GNPs induce a concentration-dependent inhibition of all three cancer cell lines. A549 cells demonstrated the lowest viability (5.11%), followed closely by MCF-7 (6.86%) at 257.8 (µg/mL), suggesting that *Lc*-GNPs exhibit the strongest anticancer activity against A549 lung cancer cells. The A549 cells exhibited the highest sensitivity to *Lc*-GNP exposure, with the lowest IC_{50} value, followed by MCF-7 and HeLa. The IC_{50} was calculated by interpolating between the two experimental points that bracketed 50% cell viability. A lower IC_{50} value indicates a higher cytotoxic potency of *Lc*-GNPs. The curve steepness (Hill coefficient) suggested a cooperative cytotoxic response, indicating effective NPs cell interactions, as shown in Figure 9.

4.8. Comparative Evaluation with Standard Anticancer Agents

The cytotoxic efficacy of *Lc*-GNPs was compared with that of standard anticancer drugs and previously reported green-synthesized GNPs (Table 5). In literature-reported information, doxorubicin IC_{50} = 1-5 µg/mL shows high potency, systemic toxicity against MCF-7 cancer cell lines, and cisplatin exhibits superior potency (IC_{50} = 2–10 µg/mL) is highly potent, nephrotoxic, and is associated with high systemic toxicity against A549. In contrast, *Lc*-GNPs show moderate cytotoxicity with excellent biocompatibility and minimal expected side effects, making

them a sustainable alternative for targeted cancer therapy. Green-synthesized GNPs derived from *Azadirachta indica* and *Aloe vera* have reported IC_{50} values of 150–300 µg/mL (MCF-7) and 120–250 µg/mL (A549), respectively. The GNPs synthesized in the present study exhibited IC_{50} values of 26.91 µg/mL (MCF-7), 45.51 µg/mL (HeLa), and 17.33 µg/mL (A549), showing strong dose-dependent cytotoxicity.

Table 3. The regression analysis data of three independent replicates of MCF-7, HeLa, and A549 cancerous cell lines with different concentrations.

S.No.	Cell line	Conc. (µg/mL)	Cell viability (%)			(Mean ± SD)
			R_1	R_2	R_3	
1	MCF-7	0.41	100	98.5	100	99.50 ± 0.87
	HeLa		98.08	99.4	92.69	96.72 ± 3.55
	A549		95.83	95.18	91.06	94.02 ± 2.59
2	MCF-7	1.23	100	95.95	95.95	97.30 ± 2.34
	HeLa		94.89	97.84	92.16	94.96 ± 2.84
	A549		87.95	88.86	94.17	90.33 ± 3.36
3	MCF-7	3.7	96.58	93.33	88.38	92.76 ± 4.13
	HeLa		94.09	89.7	91.09	91.63 ± 2.24
	A549		79.1	71.73	79.03	76.62 ± 4.24
4	MCF-7	11.11	75.61	71.58	71.57	72.92 ± 2.33
	HeLa		77.49	88.53	80.14	82.05 ± 5.76
	A549		55.37	54.34	58.85	56.19 ± 2.36
5	MCF-7	33.33	46.19	37.57	38.32	40.69 ± 4.78
	HeLa		52.69	61.15	51.96	55.27 ± 5.11
	A549		36.38	36.03	29.83	34.08 ± 3.68
6	MCF-7	100	17.53	15.73	21.03	18.10 ± 2.70
	HeLa		31.97	22.22	25.06	26.42 ± 5.01
	A549		14.27	16.51	18.76	16.51 ± 2.25
7	MCF-7	257.8	4.37	2.35	13.87	6.86 ± 6.15
	HeLa		15.75	18.18	15.63	16.52 ± 1.44
	A549		5.5	6.53	3.31	5.11 ± 1.64

Table 4. Significant results of *Lc*-GNPs against MCF-7, HeLa, and A549 cancerous cell lines.

S.No.	Concentration (µg/mL)	MCF-7 (Mean ± SD)	HeLa (Mean ± SD)	A549 (Mean ± SD)
1	0.41	96.12 ± 3.01	96.72 ± 3.55	94.02 ± 2.59
2	1.23	91.64 ± 2.88	94.96 ± 2.84	90.33 ± 3.36
3	3.70	78.42 ± 4.22	91.63 ± 2.24	76.62 ± 4.24
4	11.11	55.21 ± 3.11	71.85 ± 3.62	56.19 ± 2.36
5	33.33	35.77 ± 3.69	48.27 ± 3.94	34.08 ± 3.68
6	100	18.25 ± 2.41	26.94 ± 2.61	16.51 ± 2.25
7	257.80	6.42 ± 1.75	11.53 ± 1.86	5.11 ± 1.64
	F-Value	330.9649	212.8446	424.8923
	p-value	2.93×10^{-14}	6.23×10^{-13}	5.17×10^{-13}
	Significance/ Non Significance	Significant ($p < 0.05$)	Significant ($p < 0.05$)	Significant ($p < 0.05$)

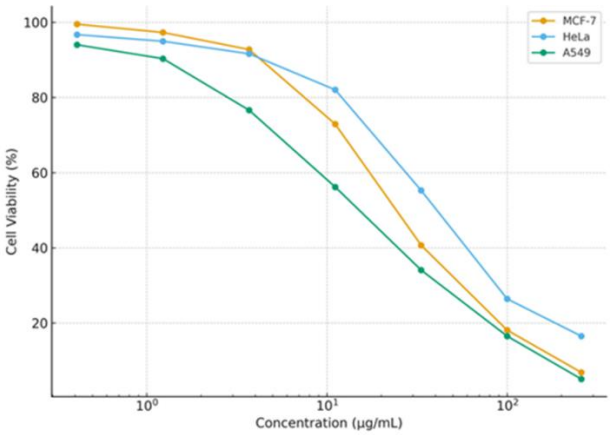

Fig. 9. Dose–response curves for Lc-GNPs on human cancer cell lines (MCF-7, HeLa, and A549) evaluated using the MTS assay. (mean ± SD, n = 3; $p < 0.05$).

Table 5. Comparative study of the present work with reported work.

S.No.	Agent/System	Cancer Cell Line	IC_{50} (µg/mL)	Remarks	Reference
			Present Work		
1	*Leucas cephalotes* GNPs	MCF-7	26.91	Green-synthesized, low toxicity (Moderate sensitivity)	Present study
2		HeLa	45.51	Effective at a given dose (Least sensitivity)	
3		A549	17.33	Strong cytotoxicity (Most sensitive)	
			(a) Reported GNPs against MCF-7 cancer cell lines		
4	*Zingiber officinale* GNPs	MCF-7	288	Moderate cytotoxicity	[69]
5	Curcumin-loaded GNPs	MCF-7	5-15	Synergistic apoptosis induction	[70]
6	PEGylated GNPs	MCF-7	80–150	Low intrinsic cytotoxicity; used for drug delivery	[71]
7	*Terminalia arjuna* GNPs	MCF-7	20–35	Strong apoptotic activity	[72]
8	*Eucalyptus globulus* GNPs	MCF-7	30–60	Moderate cytotoxicity	[73]
9	Gum arabic–capped GNPs	MCF-7	40–90	Low intrinsic toxicity	[74]
10	Chitosan–GNP conjugates	MCF-7	15–30	Positive charge → improved membrane penetration	[75]
11	*Lantadene* (*LA*) loaded GNPs	MCF-7	22–38	Phenolic-rich extract enhances activity	[76]
			(b) Reported GNPs against A549 cancer cell lines		
12	Aloe vera, Honey, *Gymnema sylvestre* GNPs	A549	120–250	Green synthesis, biocompatible	[77]
13	Chitosan-capped GNPs	A549	25–45	Enhanced uptake due to positive charge	[78]
14	*Turmeric (Curcuma longa)* GNPs	A549	25–40	ROS-mediated cytotoxicity	[79]
15	PEG–GNPs loaded with paclitaxel	A549	5–15	High potency due to drug synergy	[80]
16	*Azadirachta indica* GNPs	A549	45–80	Dose-dependent apoptosis	[81]
17	Albumin–GNP nanoconstruct	A549	20–40	Mild cytotoxicity; drug-carrier application	[82]
18	Dextran-coated GNPs	A549	60–110	Low cytotoxicity; used for imaging	[83]
			(c) Reported GNPs against HeLa cancer cell lines		
19	*Cassia auriculate* -GNPs	HeLa	50	Moderate cytotoxicity	[84]
20	*Piper nigrum* (Black pepper)-GNPs	HeLa	25–45	Good cellular uptake due to alkaloids	[85]
21	BSA-capped GNPs	HeLa	60–120	Low cytotoxicity; high stability	[86]
22	Gallic acid–reduced GNPs	HeLa	80-85	Moderate anticancer activity	[87]
23	*Ocimum tenuiflorum* GNPs	HeLa	50–90	Moderate cytotoxicity	[88]

GNPs perform promising cytotoxicity (highest Sensitivity) against A549 cancer cell lines. Thus, the Lc-GNPs demonstrate comparable or superior anticancer (breast, cervical, and lung cancer) efficacy, validating the potential of Lc as a novel and eco-friendly bio-resource for NPs-based therapeutics. Previous research indicates that the facile production, customizable surface functionalization, variable size and shape, and superior biocompatibility of GNPs have made them an attractive option for cancer treatment. This suggests that the developed GNPs can serve as a promising natural platform against carcinogenic with reduced side effects relative to conventional agents.

5. Conclusions

In this study, gold nanoparticles were successfully synthesized using *Lc* leaf extract via a simple, eco-friendly, and reproducible green synthesis route. The formation of GNPs was confirmed through UV–Vis (SPR), FTIR, DLS, XRD, SEM, and EDX analyses. The cytotoxic potential of the synthesized *Lc*-GNPs (20nm) was assessed against three human cancer cell lines, MCF-7 (breast), HeLa (cervical), and A549 (lung), using the MTS assay. Statistical analysis using one-way ANOVA followed by ($p < 0.05$) confirmed significant differences between treated and control groups, giving significant results at higher concentrations. Among the three cell lines, A549 (Cell viability: 5.11%; IC_{50} values: 17.33 µg/mL) exhibited the strongest response, followed by MCF-7 and HeLa. A lower IC_{50} value indicates a higher cytotoxic potency of *Lc*-GNPs. Overall, this work establishes *Lc* as a promising new bioresource for the green synthesis of GNPs with significant anticancer potential. Future research will focus on in vivo validation and also **on** combinatorial drug delivery approaches to further explore their nano-medical science applications.

Acknowledgements

The present author is grateful to the G.B. Pant University and Uttaranchal University for their constant encouragement throughout this work.

Funding Statement

This research received no specific grant from any funding agency.

Conflicts of interest

The authors declare that they have no known competing financial interests or personal relationships that could have appeared to influence the work reported in this paper.

Authors contribution statement

Ajay Kumar (Corresponding Author First) conceived the research idea, designed the methodology, analyzed the data, reviewed, and provided critical suggestions for improvement. **Sarvesh Rustagi** (Corresponding Author Second) analyzed the data, literature review, and assisted in theoretical derivations. **Manish Pant** contributed to data collection, **Dhruv Mishra** literature review, and assisted in theoretical derivations. **Gurleen Kaur** and **Rupinder Kaur** supported the result interpretation and validation. **Dharmendra Kumar** and **Benjamin K. Blamah** contributed to data curation, figure preparation, and technical editing. **Devendra Singh** developed the theoretical framework and prepared the original draft of the manuscript. All data included in this paper are available upon request by contacting the corresponding author.

References

[1] Smalley, K.S.M. and Herlyn, M., 2006. Towards the targeted therapy of melanoma. *Mini reviews in medicinal chemistry*, *6*(4), pp.387-393.

[2] Firer, M. A. and Gellerman, G. 2012. Targeted drug delivery for cancer therapy: the other side of antibodies. *Journal of hematology & oncology*, 5, pp.1-16.

[3] Gowda, R., Jones, N. R., Banerjee, S. and Robertson, G. P. 2013. Use of nanotechnology to develop multi-drug inhibitors for cancer therapy. *Journal of nanomedicine & nanotechnology*, 4(6), p.184.

[4] Wang, R., Billone, P. S. and Mullett, W. M. 2013. Nanomedicine in action: an overview of cancer nanomedicine on the market and in clinical trials. *Journal of Nanomaterials*, 2013(1), p.629681.

[5] McNeil, S. E. 2009. Nanoparticle therapeutics: a personal perspective. *Wiley Interdisciplinary Reviews: Nanomedicine and Nanobiotechnology*, 1(3), pp.264-271.

[6] Arvizo, R. R., Bhattacharyya, S., Kudgus, R. A., Giri, K., Bhattacharya, R. and Mukherjee, P. 2012. Intrinsic therapeutic applications of noble metal nanoparticles: past, present and future. *Chemical Society Reviews*, 41(7), pp.2943-2970.

[7] Ali Dheyab, M., Aziz, A. A. and Jameel, M. S. 2021. Recent advances in inorganic nanomaterials synthesis using sonochemistry: a comprehensive review on iron oxide, gold and iron oxide coated gold nanoparticles. *Molecules*, *26*(9), p.2453.

[8] Vinardell, M. P. and Mitjans, M. 2015. Antitumor activities of metal oxide nanoparticles. *Nanomaterials,* 5(2), pp.1004-1021.

[9] Jagadeeshan, S. and Parsanathan, R. 2021. Metal Oxides as Anticancer Agents. In *Metal, Metal Oxides and Metal Sulphides for Biomedical Applications* (pp. 281-299). Cham: Springer International Publishing.

[10] Kumar, A., Bisht, G., Siddiqui, N., Masroor, S., Mehtab, S. and Zaidi, M. G. H. 2019. Synthesis of magnetic hydrogels for target delivery of doxorubicin. *Advanced Science, Engineering and Medicine*, 11(11), pp.1071-1074.

[11] Thevenot, P., Cho, J., Wavhal, D., Nair, A., Timmons, R. B. and Tang, L. 2017. Surface chemistry influences cancer killing effect of TiO_2 nanoparticles. In Nanomedicine in Cancer (pp. 411-439). Jenny Stanford Publishing.

[12] Wason, M. S., Colon, J., Das, S., Seal, S., Turkson, J., Zhao, J. and Baker, C. H. 2013. Sensitization of pancreatic cancer cells to radiation by cerium oxide nanoparticle-induced ROS production. *Nanomedicine: Nanotechnology, Biology and Medicine*, 9(4), pp.558-569.

[13] Barabadi, H., Alizadeh, A., Ovais, M., Ahmadi, A., Shinwari, Z. K. and Saravanan, M. 2018. Efficacy of green nanoparticles against cancerous and normal cell lines: a systematic review and meta-analysis. IET nanobiotechnology, 12(4), pp.377-391.

[14] Connor, E. E., Mwamuka, J., Gole, A., Murphy, C. J. and Wyatt, M. D. 2005. Gold nanoparticles are taken up by human cells but do not cause acute cytotoxicity. *Small*, 1(3), pp.325-327.

[15] Joshi, H.C., Kharkwal, H., Kumar, A. and Gupta, P.K., 2023. Development of a quartz crystal microbalance-based immunosensor for the early detection of mesothelin in cancer. *Sensors International*, 4, p.100248.

[16] Zhu, J. W., Charkhchi, P., Adekunte, S. and Akbari, M. R. 2023. What is known about breast cancer in young women?. *Cancers*, 15(6), 1917.

[17] Barabadi, H., Alizadeh, A., Ovais, M., Ahmadi, A., Shinwari, Z. K. and Saravanan, M. 2018. Efficacy of green nanoparticles against cancerous and normal cell lines: a systematic review and meta-analysis. *IET nanobiotechnology*, 12(4), pp.377-391.

[18] Tomar, A. and Garg, G. 2013. Short review on application of gold nanoparticles. *Global Journal of Pharmacology*, 7(1), pp.34-38.

[19] BarathManiKanth, S., Kalishwaralal, K., Sriram, M., Pandian, S. R. K., Youn, H. S., Eom, S. and Gurunathan, S. 2010. Anti-oxidant effect of gold nanoparticles restrains hyperglycemic conditions in diabetic mice. *Journal of nanobiotechnology*, 8, pp.1-15.

[20] Alomari, G., Hamdan, S. and Al-Trad, B. 2021. Gold nanoparticles as a promising treatment for diabetes and its complications: Current and future potentials. *Brazilian Journal of Pharmaceutical Sciences*, 57, e19040.

[21] Ranjitha, V. R. and Ravishankar Rai, V. 2021. Bioassisted synthesis of gold nanoparticles from Saccharomonospora glauca: toxicity and biocompatibility study. *BioNanoScience*, 11(2), pp.371-379.

[22] Alhalili, Z. 2023. Metal oxides nanoparticles: general structural description, chemical, physical, and biological synthesis methods, role in pesticides and heavy metal removal through wastewater treatment. *Molecules*, 28(7), 3086.

[23] Patil, T., Gambhir, R., Vibhute, A. and Tiwari, A. P. 2023. Gold nanoparticles: synthesis methods, functionalization and biological applications. *Journal of Cluster Science*, 34(2), pp.705-725.

[24] Dikshit, P.K., Kumar, J., Das, A.K., Sadhu, S., Sharma, S., Singh, S., Gupta, P.K. and Kim, B.S., 2021. Green synthesis of metallic nanoparticles: Applications and limitations. *Catalysts*, *11*(8), p.902.

[25] Clarance, P., Luvankar, B., Sales, J., Khusro, A., Agastian, P., Tack, J.C., Al Khulaifi, M.M., Al-Shwaiman, H.A., Elgorban, A.M., Syed, A. and Kim, H.J., 2020. Green synthesis and characterization of gold nanoparticles using endophytic fungi Fusarium solani and its in-vitro anticancer and biomedical applications. *Saudi Journal of Biological Sciences*, *27*(2), pp.706-712.

[26] Bharadwaj, K.K., Rabha, B., Pati, S., Sarkar, T., Choudhury, B.K., Barman, A., Bhattacharjya, D., Srivastava, A., Baishya, D., Edinur, H.A. and Abdul Kari, Z., 2021. Green synthesis of gold nanoparticles using plant extracts as beneficial prospect for cancer theranostics. *Molecules*, *26*(21), p.6389.

[27] Roychoudhury, A. 2020. Yeast-mediated green synthesis of nanoparticles for biological applications. *Indian J Pharm Biol Res*, 8(03), pp.26-31.

[28] Santhosh, P. B., Genova, J. and Chamati, H. 2022. Green synthesis of gold nanoparticles: An eco-friendly approach. *Chemistry*, 4(2), pp.345-369.

[29] Brar, K.K., Magdouli, S., Othmani, A., Ghanei, J., Narisetty, V., Sindhu, R., Binod, P., Pugazhendhi, A., Awasthi, M.K. and Pandey, A., 2022. Green route for recycling of low-cost waste resources for the biosynthesis of nanoparticles (NPs) and nanomaterials (NMs)-A review. *Environmental Research*, *207*, p.112202.

[30] Rónavári, A., Igaz, N., Adamecz, D.I., Szerencsés, B., Molnar, C., Kónya, Z., Pfeiffer, I. and Kiricsi, M., 2021. Green silver and gold nanoparticles: Biological synthesis approaches and potentials for biomedical applications. *Molecules*, *26*(4), p.844.

[31] Osman, A.I., Zhang, Y., Farghali, M., Rashwan, A.K., Eltaweil, A.S., Abd El-Monaem, E.M., Mohamed, I.M., Badr, M.M., Ihara, I., Rooney, D.W. and Yap, P.S., 2024. Synthesis of green nanoparticles for energy, biomedical, environmental, agricultural, and food applications: A review. *Environmental Chemistry Letters*, 22(2), pp.841-887.

[32] Ahmad, T., Iqbal, J., Bustam, M. A., Irfan, M. and Asghar, H. M. A. 2021. A critical review on phytosynthesis of gold nanoparticles: Issues, challenges and future perspectives. *Journal of Cleaner Production*, 309, p.127460.

[33] Mikhailova, E. O. 2021. Gold nanoparticles: Biosynthesis and potential of biomedical application. *Journal of Functional Biomaterials*, 12(4), p.70.

[34] Sargazi, S., Laraib, U., Er, S., Rahdar, A., Hassanisaadi, M., Zafar, M.N., Díez-Pascual, A.M. and Bilal, M., 2022. *Application of green gold nanoparticles in cancer therapy and diagnosis. Nanomaterials 2022; 12: 1102* [online]

[35] Dzimitrowicz, A., Berent, S., Motyka, A., Jamroz, P., Kurcbach, K., Sledz, W. and Pohl, P. 2019. Comparison of the characteristics of gold nanoparticles synthesized using aqueous plant extracts and natural plant essential oils of Eucalyptus globulus and Rosmarinus officinalis. *Arabian Journal of Chemistry*, *12*(8), pp.4795-4805.

[36] Javed, R., Zia, M., Naz, S., Aisida, S.O., Ain, N.U. and Ao, Q., 2020. Role of capping agents in the application of nanoparticles in biomedicine and environmental remediation: recent trends and future prospects. *Journal of Nanobiotechnology*, 18(1), p.172.

[37] Aljabali, A.A., Obeid, M.A., Bashatwah, R.M., Qnais, E., Gammoh, O., Alqudah, A., Mishra, V., Mishra, Y., Khan, M.A., Parvez, S. and El-Tanani, M., 2025. Phytochemicals in cancer therapy: a structured review of mechanisms, challenges, and progress in personalized treatment. *Chemistry & Biodiversity*, 22(8), p.e202402479.

[38] Virmani, I., Sasi, C., Priyadarshini, E., Kumar, R., Sharma, S.K., Singh, G.P., Pachwarya, R.B., Paulraj, R., Barabadi, H., Saravanan, M. and Meena, R., 2020. Comparative anticancer potential of biologically and chemically synthesized gold nanoparticles. *Journal of Cluster Science*, 31(4), pp.867-876.

[39] Pang, Z., Yan, W., Yang, J., Li, Q., Guo, Y., Zhou, D. and Jiang, X., 2022. Multifunctional gold nanoclusters for effective targeting, near-infrared fluorescence imaging, diagnosis, and treatment of cancer lymphatic metastasis. *ACS nano*, 16(10), pp.16019-16037.

[40] Edris, A., Abdelrahman, M., Osman, W., Sherif, A.E., Ashour, A., Garelnabi, E.A., Ibrahim, S.R., Bafail, R., Samman, W.A., Ghazawi, K.F. and Mohamed, G.A., 2023. Design of novel letrozole analogues targeting aromatase for breast cancer: molecular docking, molecular dynamics, and theoretical studies on gold nanoparticles. *Metabolites*, 13(5), p.583.

[41] Shahidi, M., Abazari, O., Dayati, P., Bakhshi, A., Rasti, A., Haghiralsadat, F., Naghib, S.M. and Tofighi, D., 2022. Aptamer-functionalized chitosan-coated gold nanoparticle complex as a suitable targeted drug carrier for improved breast cancer treatment. *Nanotechnology Reviews*, 11(1), pp.2875-2890.

[42] Utpal, B.K., Bouenni, H., Zehravi, M., Sweilam, S.H., Mortuza, M.R., Arjun, U.V.N.V., Shanmugarajan, T.S., Mahesh, P.G., Roja, P., Dodda, R.K. and Thilagam, E., 2025. Exploring natural products as apoptosis modulators in cancers: Insights into natural product-based therapeutic strategies. *Naunyn-Schmiedeberg's Archives of Pharmacology*, pp.1-26.

[43] Yin, S., Liu, J., Kang, Y., Lin, Y., Li, D. and Shao, L., 2019. Interactions of nanomaterials with ion channels and related mechanisms. *British journal of pharmacology*, 176(19), pp.3754-3774.

[44] Wani, A.K., Akhtar, N., Mir, T.U.G., Singh, R., Jha, P.K., Mallik, S.K., Sinha, S., Tripathi, S.K., Jain, A., Jha, A. and Devkota, H.P., 2023. Targeting apoptotic pathway of cancer cells with phytochemicals and plant-based nanomaterials. *Biomolecules*, 13(2), p.194.

[45] Rosyidah, A.L., Kerdtoob, S., Yudhistyra, W.I. and Munfadlila, A.W., 2023. Gold nanoparticle-based drug nanocarriers as a targeted drug delivery system platform for cancer therapeutics: a systematic review. *Gold Bulletin*, 56(3), pp.121-134.

[46] Rajeshkumar, S., Sherif, M.H., Malarkodi, C., Ponnanikajamideen, M., Arasu, M.V., Al-Dhabi, N.A. and Roopan, S.M., 2021. Cytotoxicity behaviour of response surface model optimized gold nanoparticles by utilizing fucoidan extracted from padina tetrastromatica. *Journal of Molecular Structure*, 1228, p.129440.

[47] Mohan, U.P., Sriram, B., Panneerselvam, T., Devaraj, S., MubarakAli, D., Parasuraman, P., Palanisamy, P., Premanand, A., Arunachalam, S. and Kunjiappan, S., 2020. Utilization of plant-derived Myricetin molecule coupled with ultrasound for the synthesis of gold nanoparticles against breast cancer. *Naunyn-Schmiedeberg's Archives of Pharmacology*, 393(10), pp.1963-1976.

[48] Devi, L., Gupta, R., Jain, S.K., Singh, S. and Kesharwani, P., 2020. Synthesis, characterization and in vitro assessment of colloidal gold nanoparticles of Gemcitabine with natural polysaccharides for treatment of breast cancer. *Journal of Drug Delivery Science and Technology*, 56, p.101565.

[49] Al-Radadi, N.S., 2021. Green biosynthesis of flaxseed gold nanoparticles (Au-NPs) as potent anti-cancer agent against breast cancer cells. *Journal of Saudi Chemical Society*, 25(6), p.101243.

[50] Roh, Y.H., Eom, J.Y., Choi, D.G., Moon, J.Y., Shim, M.S. and Bong, K.W., 2021. Gold nanorods-encapsulated thermosensitive drug carriers for NIR light-responsive anticancer therapy. *Journal of Industrial and Engineering Chemistry*, 98, pp.211-216.

[51] Rahman, M., Khan, J.A., Kanwal, U., Awan, U.A. and Raza, A., 2021. Methotrexate-loaded PEGylated gold nanoparticles as hemocompatible and pH-responsive anticancer drug nanoconjugate. *Journal of Nanoparticle Research*, 23(8), p.195.

[52] Algotiml, R., Gab-Alla, A., Seoudi, R., Abulreesh, H.H., Ahmad, I. and Elbanna, K., 2022. Anticancer and antimicrobial activity of red sea seaweeds extracts-mediated gold nanoparticles. *J Pure Appl Microbiol*, 16(1), pp.207-225.

[53] El-Rafie, H.M., El-Aziz, S.M.A. and Zahran, M.K., 2023. In vitro cytotoxicity against breast cancer using biogenically synthesized gold and iron oxide nanoparticles derived from the hydroethanolic extract of Salvia officinalis L. *Chemical Papers*, 77(1), pp.361-373.

[54] Naveena, A., Jeyasundari, J., Vengatesh, P.P. and Sakthiathithan, A.S., 2023. In-vitro Anticancer Potential of Phytogenic Ag-Au Bimetallic Nanoparticles using Clitoria ternatea Flower Extract. *International Journal of Pharmaceutical Sciences and Drug Research*, 15(4), pp.432-436.

[55] Salarvand, A., Shanei, A., Hejazi, S.H., Kakhki, N.A., Abharian, P.H. and Najafizade, N., 2024. In Vitro Study of Sonodynamic Therapy Using Gemcitabine-Loaded PEG-Gold Nanoparticles Against MCF-7 Breast Cancer Cells. *Bionanoscience*, 14(3), pp.2117-2130.

[56] Nosrati-Oskouie, M., Salavatizadeh, M., Aghili-Moghaddam, N.S., Sathyapalan, T., Kesharwani, P., Tarighat-Esfanjani, A. and Sahebkar, A., 2025. Folate-Modified Curcumin-Loaded Nanoparticles for Overcoming Delivery Challenges in Cancer Treatment: A Narrative Review. *Current Pharmaceutical Biotechnology*, 26(10), pp.1423-1440.

[57] Kadam, A., Patil, R., Mahalunkar, S., Ashokkumar, M., Chauhan, R. and Gosavi, S., 2025. Liquid crystal-based optical platform for the detection of colon and breast cancer cell lines using folic acid-conjugated gold nanoparticles. *Sensors & Diagnostics*.

[58] Islam, M.M., Kaur, H., Kaur, H., Singh, S.K., Kalita, J., Kumar, A. and Singh, A., 2025. Nanotechnology in Anti-EGFR Treatments: Enhancing Delivery and Minimizing Toxicity in Cancer Therapy. *Clinical Cancer Drugs*, 11(1), p.E2212697X377694.

[59] Niżnik, Ł., Noga, M., Kobylarz, D., Frydrych, A., Krośniak, A., Kapka-Skrzypczak, L. and Jurowski, K., 2024. Gold nanoparticles (AuNPs)—toxicity, safety and green synthesis: a critical review. *International Journal of Molecular Sciences*, 25(7), p.4057.

[60] Jayeoye, T.J., Nwude, E.F., Singh, S., Prajapati, B.G., Kapoor, D.U. and Muangsin, N., 2024. Sustainable synthesis of gold nanoparticles for drug delivery and cosmeceutical applications: a review. *BioNanoScience*, 14(3), pp.3355-3384.

[61] Cory, A.H., Owen, T.C., Barltrop, J.A. and Cory, J.G., 1991. Use of an aqueous soluble tetrazolium/formazan assay for cell growth assays in culture. *Cancer communications*, 3(7), pp.207-212.

[62] Riss, T.L., Moravec, R.A., Niles, A.L., Duellman, S., Benink, H.A., Worzella, T.J. and Minor, L. "Cell viability assays." Assay guidance manual [Internet]. Available at: https://www.ncbi.nlm.nih.gov/books/NBK144065/.(May,2016)

[63] Motulsky, H. and Christopoulos, A., 2004. Fitting models to biological data using linear and nonlinear regression: a practical guide to curve fitting. *Oxford University Press*.

[64] Ritz, C., Baty, F., Streibig, J.C. and Gerhard, D., 2015. Dose-response analysis using R. *PloS one*, 10(12), p.e0146021.
[65] Mustafa, D. E., Yang, T., Xuan, Z., Chen, S., Tu, H. and Zhang, A., 2010. Surface plasmon coupling effect of gold nanoparticles with different shape and size on conventional surface plasmon resonance signal. *Plasmonics*, *5*(3), pp.221-231.
[66] Hong, X. and Hall, E.A., 2012. Contribution of gold nanoparticles to the signal amplification in surface plasmon resonance. *Analyst*, 137(20), pp.4712-4719.
[67] Andreani, A.S., Zahro, S.U., Vidiawati, A. and Fathoni, A., 2025. Colorimetric Detection of NS1 Antigen Using Functionalized Gold Nanoparticles. *Analytical and Bioanalytical Chemistry Research*, 12(4), pp.457-472.
[68] Husen, A., 2017. Gold nanoparticles from plant system: synthesis, characterization and their application. In Nanoscience and plant–soil systems (pp. 455-479). *Cham: Springer International Publishing.*
[69] Fouda, A., Eid, A.M., Guibal, E., Hamza, M.F., Hassan, S.E.D., Alkhalifah, D.H.M. and El-Hossary, D., 2022. Green synthesis of gold nanoparticles by aqueous extract of Zingiber officinale: characterization and insight into antimicrobial, antioxidant, and in vitro cytotoxic activities. *Applied Sciences*, 12(24), p.12879.
[70] Khandelwal, P., Alam, A., Choksi, A., Chattopadhyay, S. and Poddar, P., 2018. Retention of anticancer activity of curcumin after conjugation with fluorescent gold quantum clusters: An in vitro and in vivo xenograft study. *ACS omega*, 3(5), pp.4776-4785.
[71] Salarvand, A., Shanei, A., Hejazi, S.H., Abedi, I. and Kakhki, N.A., 2025. In vitro Investigation of radiotherapy along with gemcitabine loaded PEG gold nanoparticles against MCF-7 breast cancer cells. *Advanced Biomedical Research*, 14(1), p.12.
[72] Majoumouo, M.S., Sharma, J.R., Sibuyi, N.R., Tincho, M.B., Boyom, F.F. and Meyer, M., 2020. Synthesis of biogenic gold nanoparticles from Terminalia mantaly extracts and the evaluation of their in vitro cytotoxic effects in cancer cells. *Molecules*, 25(19), p.4469.
[73] Pinto, R.J., Lucas, J.M., Morais, M.P., Santos, S.A., Silvestre, A.J., Marques, P.A. and Freire, C.S., 2017. Demystifying the morphology and size control on the biosynthesis of gold nanoparticles using Eucalyptus globulus bark extract. *Industrial Crops and Products*, 105, pp.83-92.
[74] Selim, M.E. and Hendi, A.A., 2012. Gold nanoparticles induce apoptosis in MCF-7 human breast cancer cells. *Asian Pacific Journal of Cancer Prevention*, 13(4), pp.1617-1620.
[75] Martínez-Torres, A.C., Zarate-Triviño, D.G., Lorenzo-Anota, H.Y., Ávila-Ávila, A., Rodríguez-Abrego, C. and Rodríguez-Padilla, C., 2018. Chitosan gold nanoparticles induce cell death in HeLa and MCF-7 cells through reactive oxygen species production. *International journal of nanomedicine*, pp.3235-3250.
[76] Jaafar, N.D., Al-Saffar, A.Z. and Yousif, E.A., 2020. Genotoxic and cytotoxic activities of lantadene A-loaded gold nanoparticles (LA-AuNPS) in MCF-7 cell line: an in vitro assessment. *International journal of toxicology*, 39(5), pp.422-432.
[77] Malik, S., Niazi, M., Khan, M., Rauff, B., Anwar, S., Amin, F. and Hanif, R., 2023. Cytotoxicity study of gold nanoparticle synthesis using Aloe vera, honey, and Gymnema sylvestre leaf extract. *ACS omega*, 8(7), pp.6325-6336.
[78] Choi, S.Y., Jang, S.H., Park, J., Jeong, S., Park, J.H., Ock, K.S., Lee, K., Yang, S.I., Joo, S.W., Ryu, P.D. and Lee, S.Y., 2012. Cellular uptake and cytotoxicity of positively charged chitosan gold nanoparticles in human lung adenocarcinoma cells. *Journal of Nanoparticle Research*, 14(12), p.1234.
[79] Dutta, S., Mitra, S.K., Bir, A., TR, P., Ghosh, A., DUTTA, S. and MITRA, S.K., 2023. Enhancing anti-cancer activity: green synthesis and cytotoxicity evaluation of turmeric-gold nanocapsules on A549 lung cancer cells. *Cureus*, 15(8).
[80] Heo, D.N., Yang, D.H., Moon, H.J., Lee, J.B., Bae, M.S., Lee, S.C., Lee, W.J., Sun, I.C. and Kwon, I.K., 2012. Gold nanoparticles surface-functionalized with paclitaxel drug and biotin receptor as theranostic agents for cancer therapy. *Biomaterials*, 33(3), pp.856-866.
[81] Bin-Jumah, M.N., Al-Abdan, M., Al-Basher, G. and Alarifi, S., 2020. Molecular mechanism of cytotoxicity, genotoxicity, and anticancer potential of green gold nanoparticles on human liver normal and cancerous cells. *Dose-Response*, 18(2), p.1559325820912154.
[82] Chen, Y., Liu, S., Liao, Y., Yang, H., Chen, Z., Hu, Y., Fu, S. and Wu, J., 2023. Albumin-modified gold nanoparticles as novel radiosensitizers for enhancing lung cancer radiotherapy. *International Journal of Nanomedicine*, pp.1949-1964.
[83] Brown, S.D., Nativo, P., Smith, J.A., Stirling, D., Edwards, P.R., Venugopal, B., Flint, D.J., Plumb, J.A., Graham, D. and Wheate, N.J., 2010. Gold nanoparticles for the improved anticancer drug delivery of the active component of oxaliplatin. *Journal of the American Chemical Society*, 132(13), pp.4678-4684.
[84] Priya Tharishini, P.S.N.C., Saraswathy, N.C., Smila, K.H., Yuvaraj, D., Chandran, M. and Vivek, P., 2014. Green synthesis of gold nano particles from Cassia auriculata leaf aqueous extract and its cytotoxicity effect on in vitro cell line. *Int. J. ChemTech Res*, 6(9), pp.4241-4250.
[85] Muddapur, U.M., Alshehri, S., Ghoneim, M.M., Mahnashi, M.H., Alshahrani, M.A., Khan, A.A., Iqubal, S.S., Bahafi, A., More, S.S., Shaikh, I.A. and Mannasaheb, B.A., 2022. Plant-based synthesis of gold nanoparticles and theranostic applications: a review. *Molecules*, 27(4), p.1391.
[86] Abdulateef, S.A., Raypah, M.E., Omar, A.F., Jafri, M.M., Ahmed, N.M., Kaus, N.H.M., Seeni, A., Mail, M.H., Tabana, Y., Ahmed, M. and Al Rawashdah, S., 2023. Rapid synthesis of bovine serum albumin-conjugated gold nanoparticles using pulsed laser ablation and their anticancer activity on hela cells. *Arabian Journal of Chemistry*, 16(1), p.104395.
[87] You, B.R., Moon, H.J., Han, Y.H. and Park, W.H., 2010. Gallic acid inhibits the growth of HeLa cervical cancer cells via apoptosis and/or necrosis. *Food and Chemical Toxicology*, 48(5), pp.1334-1340.
[88] Bharadwaj, K.K., Rabha, B., Pati, S., Sarkar, T., Choudhury, B.K., Barman, A., Bhattacharjya, D., Srivastava, A., Baishya, D., Edinur, H.A. and Abdul Kari, Z., 2021. Green synthesis of gold nanoparticles using plant extracts as beneficial prospect for cancer theranostics. *Molecules*, 26(21), p.6389.